Int. J. Electrochem. Sci., 8 **(2013)** 914 - 923

International Journal of
ELECTROCHEMICAL
SCIENCE
www.electrochemsci.org

XRD, SEM and XAS Studies of FeCo Films Electrodeposited at Different Current Density

Wei Lu[*], *Ping Huang, Chenchong He and Biao Yan*

School of Materials Science and Engineering, Shanghai Key Lab. of D&A for Metal-Functional Materials, Tongji University, Shanghai 200092, China
[*]E-mail: weilu@tongji.edu.cn

Received: 11 November 2012 / *Accepted:* 4 December 2012 / *Published:* 1 January 2013

In this paper, the effect of electrodepositing current density on the composition, microstructure and electric properties of FeCo films were investigated in details by using EDS, XRD, SEM and XAS. The composition of Fe-Co films keeps nearly constant at different current densities. The deposited films have a mixed structure of fcc γ phase and bcc α-Co_7Fe_3 phase. The bcc phase is dominant in the films electrodeposited at current density less than 40 mA/cm^2 (≤40 mA/cm^2) while fcc phase is dominant in the film deposited at current density of 50 mA/cm^2. High electrodepositing current density leads to a small decrease in the lattice parameter and an increase in grain sizes for the bcc phase. At all current densities, a colony-like morphology which consists of a lot of grain colonies having various sizes is seen. With increasing current densities (e.g., 10~20 mA/cm^2), smooth, uniform and compact electrodeposits are obtained, while at higher current densities (e.g., 30~50 mA/cm^2) the deposits are porous and cracks can be observed in the films. XAS results of the electrodeposited films indicate the presence of Fe^{3+} and Co^{2+} ions which mainly come from the surface oxidation of the as-deposited films and electrolytes.

Keywords: FeCo film; electrochemical deposition; current density

1. INTRODUCTION

Ferromagnetic nanocrystalline FeCo alloys are used in the fabrication of high areal density heads, microelectromechanical systems (MEMS), and protective coatings due to their high saturation magnetic flux density and high Curie temperature [1, 2]. One of the very important properties of FeCo films is microstructure, which resulting very different in the magnetic properties. Thus, in order to improve magnetic properties of FeCo films, it is necessary to understand the origin of the microstructure.

Nowadays, in order to fabricate nanocrystalline metallic films, many deposition techniques are available, such as sputtering, molecular beam epitaxy, vacuum evaporation, sol-gel, electrodeposition and etc. But all these methods require high precision process control, which demands higher capital cost and incurs huge material waste. As compared to different deposition methods for the metallic films, electrodeposition has always been a well accepted method [3-7], due to its relatively higher efficiency, easier control and lower cost. It has an advantage of preparation of films over a large surface area without impairing materials purity in a relatively shorter period of time. During the electrodeposition process, the structural factors and properties of the deposited films are strongly affected by the deposition conditions [8-11], such as deposition temperature, electrolyte pH, current density and potential. By adjusting the electrochemical deposition parameters, it is possible to control and optimize the structure and properties of the electrodeposited films, such as thickness, grain size, phase, etc.

The authors have previously reported on the effect of electrochemical deposition temperatures on the composition and microstructure of FeCo films [12]. It shows that the composition and phase structure of the deposited Fe-Co films are greatly affected by the electrolyte temperatures. In addition, the processing of other deposition conditions, such as pH of deposition solution and composition of solution, on the microstructure and magnetic properties of FeCo films was investigated [13-15]. However, there have been very few studies which have been done on the systematic investigation of the effect of electrolytic current density on the microstructure of the electrochemical deposited FeCo alloy films. To address these issues, in this paper, we have investigated systematically the composition and microstructure evaluation in electrodeposited FeCo alloy films at different current densities in the range from 10 mA/cm^2 to 50 mA/cm^2.

2. EXPERIMENTAL

FeCo thin films were fabricated by electrodeposition from Sulfate bath using a conventional three electrode cell. The copper plate serves as the working cathode with the surface area of 1cm^2 while a graphite plate serves as the anode with much larger surface area. Prior to deposition, the substrate was first mechanically polished, then washed in 10% H_2SO_4 and distilled water. The reference electrode was a saturated calomel electrode.

Table 1. Compositions of the electrolytes and major electrodepositing parameters

Composition	pH	Temperature (^{o}C)
$CoSO_4.7H_2O$ (0.2mol/L) $FeSO_4.7H_2O$ (0.15mol/L) Na_2SO_4 (0.7mol/L) Ascorbic Acid (0.05mol/L) Boric acid (0.4mol/L)	3	RT

The compositions of the electrolytes of Co^{2+}/Fe^{2+} were shown in Table 1, together with major electrodepositing parameters. The total concentration of ferrous sulfate [$FeSO_4 \cdot 7H_2O$] and cobalt

sulfate [$CoSO_4 \cdot 7H_2O$] was kept 0.35 mol/L. All chemicals were reagent grade and dissolved in distilled water. The electrodeposition was conducted at current density from 10 mA/cm^2 to 50 mA/cm^2 with a certain stirring rate. During electrodeposition, the bath temperature is kept at room temperature (RT).

The crystallographic structure of electrodeposited FeCo films was characterized by X-ray Diffraction (XRD). The compositions of the samples were detected through energy dispersive spectrometer (EDS). Field-emission scanning electronic microscopy (FESEM) was employed to examine the morphology of the films. Soft X-ray absorption spectroscopy (XAS) measurements on electrodeposited films corresponding to the energy of Fe and Co $L_{3,2}$-edges was performed at beamline 08U of Shanghai Synchrotron Radiation Facility (SSRF).

3. RESULTS AND DISCUSSION

The composition of electrodeposited FeCo alloy films at different current densities is shown in Fig.1. As can be seen, the Fe and Co concentrations in the electrodeposited films are approximately 47.5 at.% and 52.5 at.%, respectively. The molar ratio of Co:Fe in the bath solution was 4:3, which should result in electrodeposited films with compositions of ~57 at% Co (~43 at% Fe) assuming non-preferential electrodeposition. As can be seen from above results, Fe is preferentially deposited, relative to the composition of electrolyte solution, at the expense of Co, in present study. Iron has a lower reduction potential than Cobalt. Therefore, the results indicate slightly anomalous electrodepositing behavior for the electrolyte solution at room temperature. This behavior is well established in previous studies [16-18] and is thought to be the result of an inhibiting effect of Fe on the nucleation and growth of Co on the cathode surface [18].

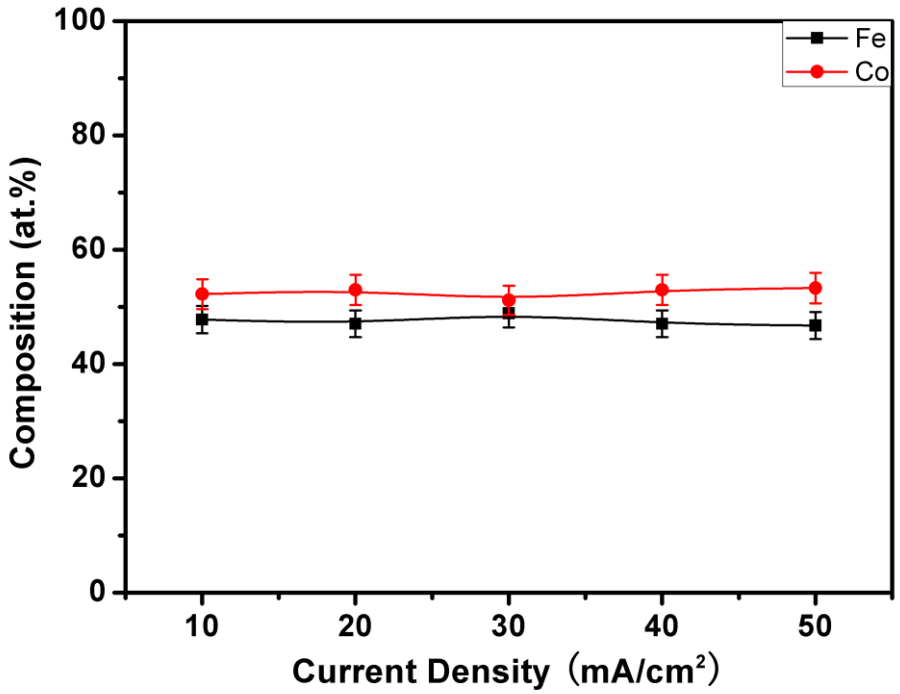

Figure 1. Compositions of Co–Fe thin films electrodeposited at different current densities

Interestingly, the Fe and Co contents in the deposited films keep almost constant when the electrodepositing current density changes in the range of 10~50 mA/cm^2. In fact, according to Brenner [19], an increase in the applied current density causes increasing the percentage of the less noble metal. However, in present study, the composition of the deposited films relatively remains constant in the current density range of 10~50 mA/cm^2. This indicates that current density (10~50 mA/cm^2) has very little influence on the contents of Fe and Co in FeCo films during the electrochemical deposition process and the reduction of Fe and Co metals at the cathode surface is mainly controlled by diffusion in present experiment.

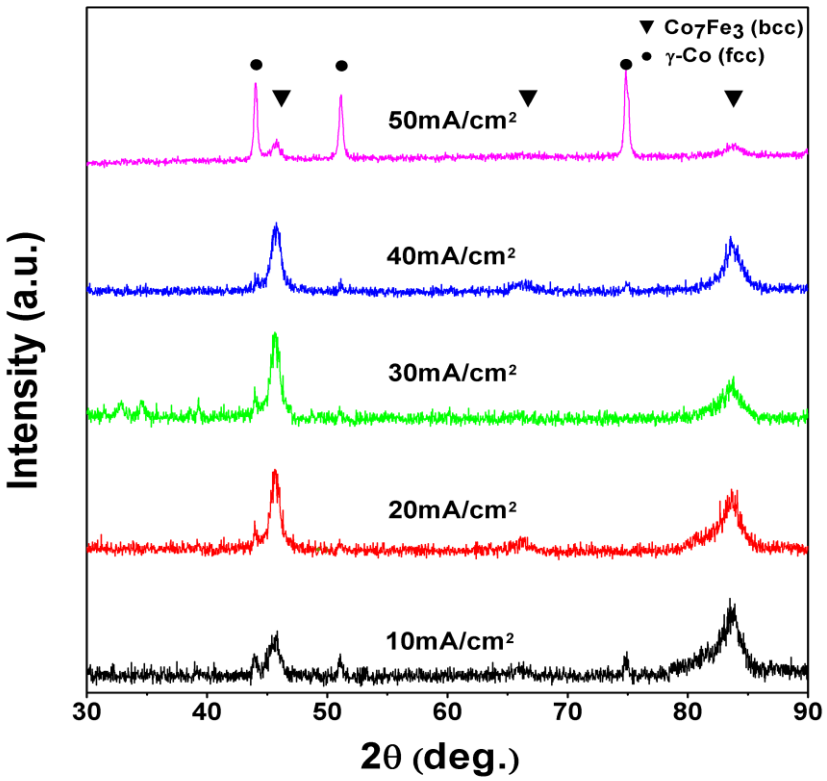

Figure 2. XRD patterns of FeCo films electrodeposited at different current densities

Fig.2 shows the XRD patterns of FeCo films electrodeposited at different current density. From the patterns, it can be seen that the films have a mixed phases of face-centered cubic (fcc) solid solution (γ phase) and body-centered cubic (bcc) α-Co_7Fe_3 phase (α-Fe type). As seen from the figure, the reflections from the characteristic (111), (200) and (220) crystal planes of fcc CoFe solid solution phase were observed at approximately 2θ=44^o, 51 ^{o} and 75^o, respectively. In addition, the (110), (200), (211) peaks of bcc α-Co_7Fe_3 phase were observed at about 45^o, 66^o and 84^o, respectively. The patterns indicate that the films electrodeposited at current densities less than 40 mA/cm^2 (≤40 mA/cm^2) have a mixed phase of fcc and bcc phases but the bcc phase is dominant. When the current density is increased to 50 mA/cm^2, the peak intensity of fcc phase increases sharply. This means that the bcc phase transforms to fcc phase and the fcc phase becomes dominant in the FeCo film. This indicates that although the Fe and Co contents did not change with different electrodepositing current density,

the different current densities indeed result in a phase transformation in the electrodeposited FeCo films.

According to the phase diagram of Fe-Co binary alloy [20], fcc solid solution phase is thermodynamically stable for high Co concentration (>90 at%) at low temperature (<700 ℃) or for all alloy concentrations at temperatures between ~985 ℃ and ~1475 ℃ while bcc α phase is stable for Fe concentrations in excess of 80 at% at temperatures below 500 ℃. The binary phase diagram gives a good indication of the phases that might be expected in Fe–Co thin films at a particular composition. However, although thermodynamically stable at low temperature and over a wide composition range (25~75 at% Fe) according to the phase diagram (Fig. 1), α' phase is never observed in our electrodeposited thin films and other researches [21-25]. It is reported [21-25] that under many electrodepositing conditions the fcc Fe-Co solid solution phase and bcc α phase form during electrodeposition. The formation of non-equilibrium phases of the two solid solution phases is not surprising for electrodeposition systems as the deposition rates do not provide sufficient time for the ordering of Co and Fe atoms on specific lattice positions to form α'-CoFe phase. In our work, for electrodeposition of FeCo films with Co concentrations keeping at around 52.5 at.% at all electrodepositing current densities, the fcc and bcc solid solution was obtained for all the samples.

Table 2. Average lattice parameters (nm) of bcc phase in FeCo films electrodeposited at different current densities

Current density (mA/cm^2) / phase	10	20	30	40	50
bcc phase	0.2830	0.2815	0.2807	0.2805	0.2801

The lattice parameters of bcc phase in the electrodeposited FeCo films were calculated based on the peak positions in the XRD patterns. Table.2 shows the average lattice parameters of bcc phase in alloy films fabricated at different current densities. Higher depositing current density leads to a small decrease in the lattice parameter for the bcc phase. It is known that the composition of electrodeposited FeCo films keeps almost constant at different current densities. It can be expected that the change of lattice parameters of bcc phase in FeCo films at different current densities is not caused by composition variations. Therefore, another possible reason for the change of lattice parameter may be raised. It is known that with increasing current density, the film thickness increases, which results in higher strains in the film. Eventually, cracking of the films can be observed in the FeCo films electrodeposited at high current density (shown in Fig.4). This indicates that there is an increasing strain in the FeCo film with increasing electrodepositing current density. The higher strains in FeCo film lead to larger lattice distortion, which results in the decrease of lattice parameter of bcc phase in deposited FeCo films.

By using Scherer equation, the averaged grain sizes of bcc phase in FeCo films electrodeposited at different current densities are calculated and shown in Fig.3. It can be seen that

with increasing current densities, the averaged grain sizes of bcc phase increase a little from around 20 nm (10 mA/cm^2) to 23 nm (40 mA/cm^2). Further increasing the current density, the bcc phase partially transforms to fcc phase and the corresponding averaged grain size of bcc phase increases sharply from around 23 nm (40 mA/cm^2) to 45 nm (40 mA/cm^2). Deposition of FeCo grains in an electrodeposition process involves two steps. The first step is the discharge of Fe and Co ions and generation of Fe and Co atoms. There are two scenarios in the growth of FeCo grains: (1) the incorporation of Fe and Co atoms into the grains and thus grain growth and (2) the formation of new nucleus when the rate of grain growth may not be sufficient to cater for generation of atom [26]. It has been shown that the critical radius of the surface nucleus is a function of the overpotential [26], the higher the overpotential is, the smaller the nucleus radius and thus the higher the nucleation rate would be. Therefore, with an increase in the current density, a higher overpotential, an accompanying increase in nucleation frequency and a reduction in the grain size could be achieved. As it was known, parameters which increase the nucleation rate would decrease the grain growth and vice versa. From above discussion, it can be possibly suggested that a special condition is governed during the deposition of FeCo films which allows an increasing grain sizes to be obtained with increasing current densities.

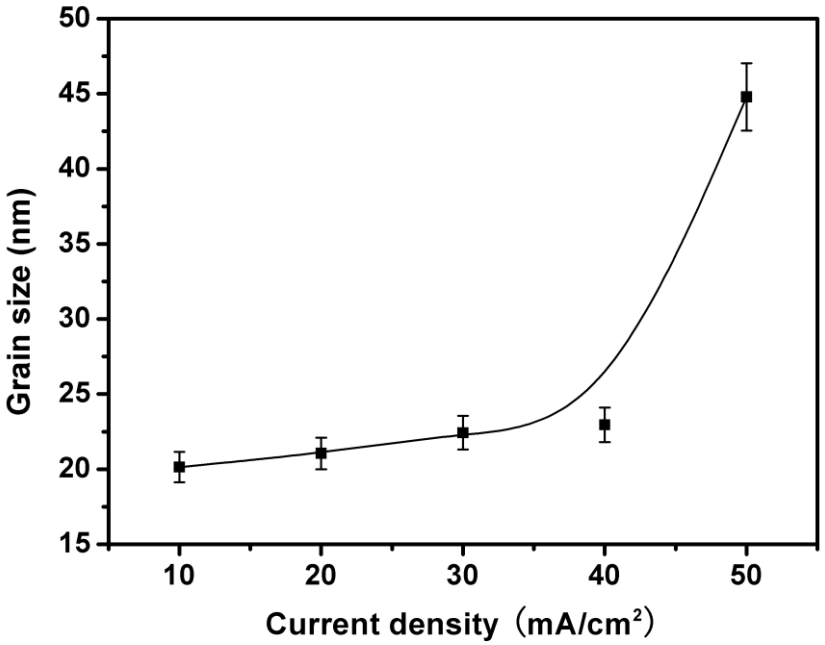

Figure 3. Averaged grain sizes of bcc phase in FeCo films electrodeposited at different current densities

Fig. 4 shows the surface morphology of FeCo films electrodeposited at various current densities ranging from 10 mA/cm^2 to 50 mA/cm^2. At all current densities, a colony-like morphology which consists of a lot of grain colonies having various sizes is seen. Each colony could be found to contain several smaller grains. With increasing current densities (e.g., 10~20 mA/cm^2), smooth, uniform and compact electrodeposits are obtained, while at higher current densities (e.g., 30~50 mA/cm^2) the deposits are porous and cracks can be observed in the films. This change in morphology can be explained in the following way. At low current densities the discharge of Fe and Co ions occurs

slowly, and hence the rate of growth of nuclei exceeds the rate at which the new ones form; the deposits obtained under these conditions should be smooth and uniform.

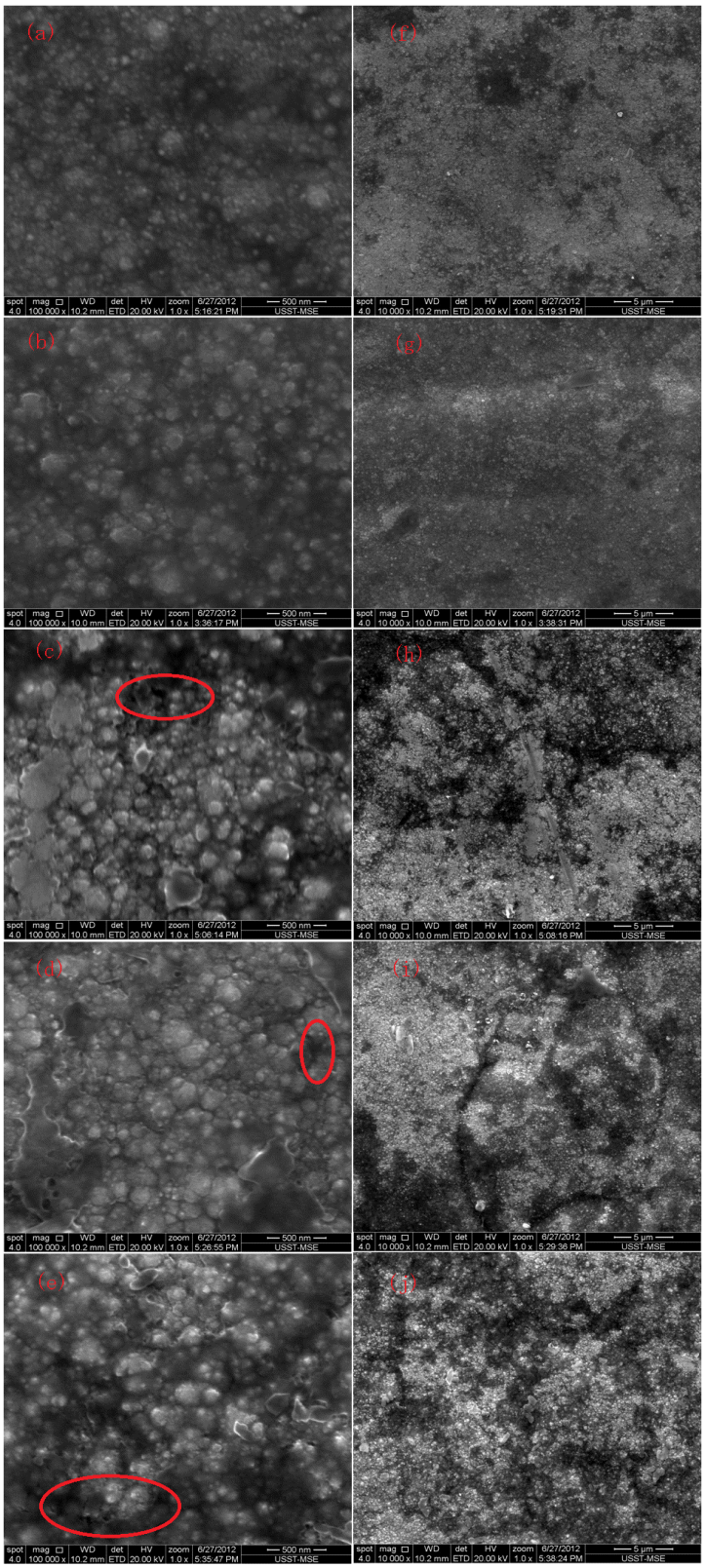

Figure 4. Surface morphology of FeCo films electrodeposited at different current densities. (a)/(f):10mA/cm^2; (b)/(g):20mA/cm^2; (c)/(h):30mA/cm^2; (d)/(i):40mA/cm^2; (e)/(j):50mA/cm^2.

However when current density exceeds a critical value, (30 mA/cm^2), a porous and non uniform microstructure develops. This can be attributed to the high overpotential, which causes the Fe and Co ions, from solution to move at a very fast rate towards cathode. This may lead to a depletion of the Fe and Co ion concentrations of the aqueous solution adjacent to the cathode and the electrode surface gets polarized. In order to overcome the concentration polarization, a greater change in potential is required to maintain the current and thus, the system enforces hydrogen ions to be discharged at a very high rate. The hydrogen evolution competes with the metal deposition as the current density increases further. The hydrogen gas evolution give rise to bubble formation that often gets incorporated in the crystal lattice resulting in porous and spongy deposits [27, 28]. The pores, as shown in the enclosed circle of Fig.4 (c, d, e), are clearly visible in the films electrodeposited at high current densities (e.g., 30~50 mA/cm^2).

Soft x-ray absorption spectroscopy (XAS) is a powerful high-energy probe to investigate the electronic structure of transition metal compounds. To investigate the influence of current density on the electronic properties of electrodeposited FeCo films, XAS experiments were performed at room temperature at the $L_{3,2}$ edges of these 3d metals. Fig. 5(a) and (b) shows Fe $L_{3,2}$ and Co $L_{3,2}$-edge spectra of FeCo films deposited at different current density. It is observed that both Fe spectra and Co spectra (Fig. 5) show multiplet spectral features for the samples electrodeposited at all current densities. The post edge peak, as shown by a down arrow in Fig.5 (a), indicates the presence of Fe^{3+} in the system. In Fig. 5(b) it is also clear that Co^{2+} ions are presented in all the samples. The presence of Fe^{3+} and Co^{2+} ions mainly come from the surface oxidation of the as-deposited films and electrolytes.

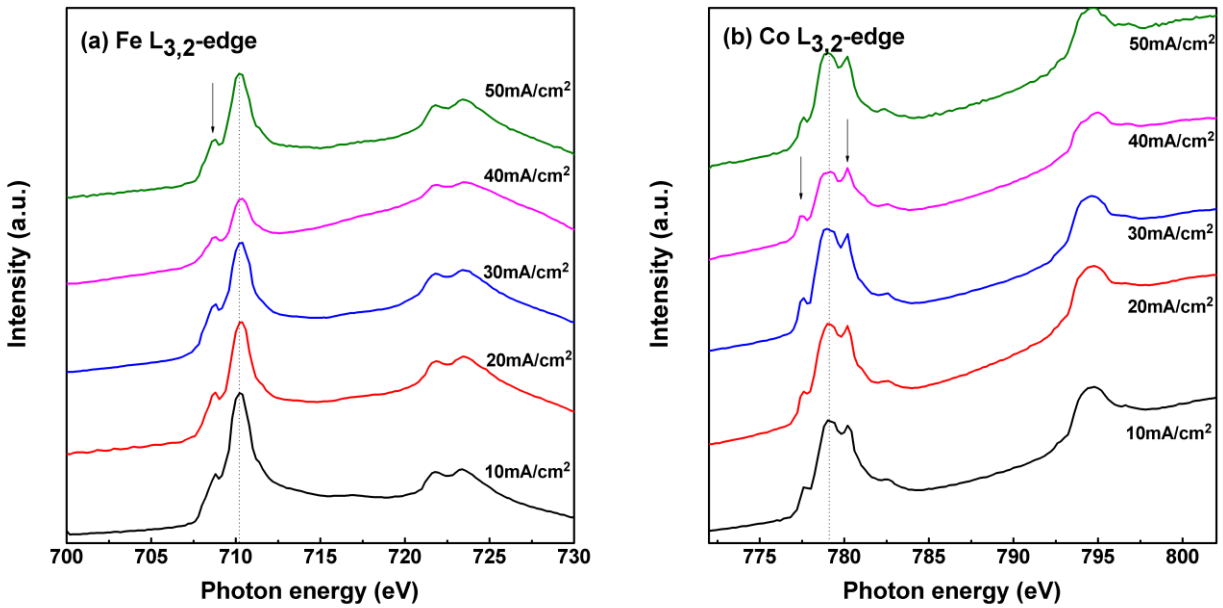

Figure 5. Fe $L_{3,2}$ and Co $L_{3,2}$-edge spectra of FeCo films deposited at different current densities

4. CONCLUSIONS

FeCo films were electrodeposited on Cu substrates at different current densities. The composition of Fe-Co films keeps nearly constant at different current densities and the reduction of Fe

and Co metals at the cathode surface is mainly controlled by diffusion in present experiment. The deposited films have a mixed structure of fcc γ phase and bcc α-Co_7Fe_3 phase. The bcc phase is dominant in the films electrodeposited at current density less than 40 mA/cm^2 (≤40 mA/cm^2) while fcc phase is dominant in the film deposited at current density of 50 mA/cm^2. High electrodepositing current density leads to a small decrease in the lattice parameter for the bcc phase. The decreasing of lattice parameter is resulted from the increasing strain in the FeCo film with increasing electrodepositing current density. It can be possibly suggested that a special condition is governed during the deposition of FeCo films which allows an increasing grain sizes to be obtained with increasing current densities. At all current densities, a colony-like morphology which consists of a lot of grain colonies having various sizes is seen. With increasing current densities (e.g., 10~20 mA/cm^2), smooth, uniform and compact electrodeposits are obtained, while at higher current densities (e.g., 30~50 mA/cm^2) the deposits are porous and cracks can be observed in the films. XAS results of the electrodeposited films indicate the presence of Fe^{3+} and Co^{2+} ions which mainly come from the surface oxidation of the as-deposited films and electrolytes.

ACKNOWLEDGEMENTS
The present work was supported by National Natural Science Foundation of China (Grant No. 50901052, 51071109) and Program for Young Excellent Talents in Tongji University (Grant No. 2009KJ003) and "Chen Guang" project (Grant No.10CG21) supported by Shanghai Municipal Education Commission and Shanghai Education Development Foundation. In addition, the authors would like to thank SSRF for the XAS measurements.

References

1. I. Shao, L.T. Romankiw, C. Bonhote, *J. Cryst. Growth*, 312 (2010) 1262
2. I. Shao, P.M. Vereecken, C.L. Chien, R.C. Cammarata, P.C. Searson, *J. Electrochem. Soc.*, 150 (2007) D572
3. G. Saravanan, S. Mohan, Int. J. Electrochem. Sci., 6 (2011) 1468
4. R.Balachandran, H.K.Yow, B.H.Ong, K.B.Tan, K.Anuar, H.Y.Wong, *Int. J. Electrochem. Sci.*, 6 (2011) 3564
5. J. A. R. Márquez, C. M. B. Rodríguez, C. M. Herrera, E. R. Rosas, O. Z. Angel, O. T. Pozos, *Int. J. Electrochem. Sci.*, 6 (2011) 4059
6. H. B. Hassan, Z. Abdel Hamid, *Int. J. Electrochem. Sci.*, 6 (2011) 5741
7. B. Bozzini, D. Lacitignola, I. Sgura, *Int. J. Electrochem. Sci.*, 6 (2011) 4553
8. J.-W. Park, J.-Y. Eom, H.-S. Kwon, *Int. J. Electrochem. Sci.*, 6 (2011) 3093
9. G. Orhan , G. Hapci, O. Keles, *Int. J. Electrochem. Sci.*, 6 (2011) 3966
10. J.C. Ballesteros, E. Chainet, P. Ozil, Y. Meas, G. Trejo, *Int. J. Electrochem. Sci.*, 6 (2011) 2632
11. H. Adelkhani, M. Ghaemi, M. Ruzbehani, *Int. J. Electrochem. Sci.*, 6 (2011) 123
12. W. Lu, P. Huang, C. He, B. Yan, *Int. J. Electrochem. Sci.*, 7 (2012), in press
13. C. Qiang, J. Xu, S. Xiao, Y. Jiao, Z. Zhang, Y. Liu, L. Tian, Z. Zhou, *Appl. Surf. Sci.*, 257 (2010) 1371
14. I. Tabakovic, S. Riemer, N. Jayaraju, V. Venkatasamy, J. Gong, *Electrochimica Acta*, 58 (2011) 25
15. X. Yang, L. Gong, J.Wei, L. Qiao, T. Wang, F. Li, *J. Phys. D: Appl. Phys,*. 43 (2010) 215002
16. X. Liu, P. Evans, G. Zangari, *IEEE Trans. Mag*., 36 (2000) 3479
17. S. Zhou, Q. Liu, D.G. Ivey, *IEEE Int. Nanoelectron. Conf*., 474 (2008) 4585531

18. R. Bertazzoli, D. Pletcher, *Electrochemica Acta*., 38 (1993) 671
19. A. Brenner, Electrodeposition of alloys, Academic press, New York (1963)
20. H. Bakar, ASM Handbook, Volume 3 Alloy Phase Diagrams, ASM international, Materials Park, Ohio (1992)
21. K. Sundaram, V. Dhanasekaran, T. Mahalingam, *Ionics*, 17 (2011) 835
22. S. Mehrizi , M. Heydarzadeh Sohi, S.A. Seyyed Ebrahimi, *Surface & Coatings Technology* 205 (2011) 4757
23. D. Zhou,M. Zhou, M. Zhu, X. Yang, M. Yue, *J. Appl. Phys.*, 111 (2012) 07A319
24. S. H. Teh, I. I.Yaacob, *IEEE Trans. Mag*., 47 (2011) 4398
25. H. Kockar, M. Alper, T. Sahin, O. Karaaga, *Journal of Magnetism and Magnetic Materials*, 322 (2010) 1095
26. Y. Li, H. Jiang, W. Huang, H. Tian, *Appl. Surf. Sci.*, 254 (2008) 6865
27. D. R. Gabe, *J. Appl. Electrochem.*, 27 (1997) 908
28. C. Fan, J. P. Celis, J. R. Roos, *J. Electrochem. Soc.*, 138 (1991) 2917